Astron. Astrophys. 80, 13–21 (1979)

ASTRONOMY AND ASTROPHYSICS

Spectral Index Dependent Properties of Steep Spectrum Radio Sources*

George Blumenthal[1] and George Miley[1,2]

[1] Lick Observatory, Board of Studies in Astronomy and Astrophysics, University of California, Santa Cruz, California, USA
[2] Sterrewacht, Huygens Laboratorium, Wassenaarsweg 78, Leiden, The Netherlands

Received August 28, 1978

Summary. The spectral index dependence of the properties of steep spectrum 3C and 4C radio sources ($\alpha \lesssim -0.5$) was investigated by determining the fractions of such sources with apparent magnitude smaller than m_0, with redshifts smaller than z_0, with 178 MHz radio luminosity smaller than P_0, and angular size larger than θ_0. Significant and similar variations in these fractions were found for both the 3C and 4C sample and for quasars and radio galaxies when spectral indices between 178 and 5000 MHz were used.

The correlations suggest that (i) the steep spectrum sources are on average further away and more luminous and (ii) the origins of the redshifts of radio galaxies and quasars are the same.

Expressions for the fractions were derived and evaluated under simplifying assumptions about the form of the radio luminosity and density evolution functions and were then compared with the observations. Small changes in the luminosity function and/or large changes in the density evolution with spectral index are needed to explain the observed effects but at present we cannot distinguish between these two causes.

The spectral index dependence of the fraction of sources with apparent magnitude smaller than m_0 exhibited a quite different behaviour for spectral indices selected below 178 MHz, showing that low frequency steep spectrum sources have different properties.

Key words: radio sources — spectral index — luminosity functions — evolution — quasars

1. Introduction

It is well known that the distribution of spectral indices for extragalactic radio sources is double peaked. The sources with flat spectra are characterized by sizes $\lesssim 1$ pc and are often variable, whereas steep spectrum sources have typical sizes of ~ 100 kpc. Steep spectrum sources are often called "normal" spectrum objects because they were the dominant population in the earliest radio surveys, carried out at meter wavelengths.

In this article we shall study some properties of relatively strong steep spectrum sources as a function of spectral index. To this end it is important to consider well defined samples which have been studied with sufficient radio resolution to determine their angular size distribution and minimize confusion effects. Such samples should embrace the widest possible range of spectral index.

Steep spectrum sources have a spectral index distribution which peaks at $\alpha \approx -0.8$ ($S \propto \nu^{\alpha}$), with a standard deviation of ~ 0.2. In an attempt to improve the statistics for very steep spectrum sources, Tielens et al. (1978) (TMW) recently defined and investigated a sample of forty-six 4C sources with $\alpha_{178}^{5000} < -1$, where α_{178}^{5000} is the spectral index measured between 178 and 5000 MHz. They found that the fraction of sources which could be identified optically is a strong function of spectral index and that the steepest spectrum sources had the smallest angular size. Also, the identification fraction of TMW's sources (defined above 178 MHz) was strikingly lower than that of a sample of 41 sources with steep spectra defined below 178 MHz studied by Slingo (1974). The behaviour of the TMW sample is qualitatively consistent with that expected from the relationship of luminosity with spectral index noted by previous authors (e.g. Heeschen, 1960; Véron et al., 1972; Macleod and Doherty, 1972; Bridle et al., 1972).

Here we shall investigate these effects in more depth and in particular compare samples of 3C and 4C sources. We shall examine the fraction of sources which have, respectively apparent magnitude, redshift, luminosity, and angular size smaller than a given value. Such fractions are useful tools for handling parameters which can be measured down to a given instrumental limit since (i) the inherent uncertainties are well determined, (ii) their values are relatively easy to evaluate from cosmological theory, (iii) several unwanted effects cancel in the fractions, and (iv) standard methods such as the V/Vm test (e.g. Schmidt, 1977) are difficult to apply when some of the redshifts are unknown.

We define:
$f(>S_0, <m_0)$ as the fraction of sources having observed 178 MHz flux densities greater than S_0 with visual magnitudes small than m_0,
$f(>S_0, <z_0)$ as the fraction of sources having observed 178 MHz flux densities greater than S_0 with redshifts smaller than z_0,
$f(>S_0, <P_0)$ as the fraction of sources having observed 178 MHz flux densities greater than S_0 with emitted 178 MHz monochromatic luminosities smaller than P_0,
$f(<S_0, >\theta_0)$ as the fraction of sources having observed

Send offprint requests to: G. Miley[2]
* *Lick Observatory Bulletin* No. 816.

Table 1. The 3C sample according to α_{178}^{1400}

α_{178}^{1400}, range	(-.15,-.48)	(-.50,-.73)	(-.74,-.82)	(-.83,-.88)	(-.89,-.99)	(-.99,-1.31)
Sources, 3C	84,138,231, 286,287,345, 454.3	19,20,31, 33,41,48, 49,67,147, 153,184.1,269.1, 268.3,272.1,293, 295,309.1,321, 326,330,334, 336,337,343, 343.1,346,380, 382,386,390.3, 449	33.1,42,43, 65,76.1,83.1B, 98,123,132, 192,196,223, 236,245,264, 268.4,274, 277.3,280,299, 303,315,318, 325,340,349, 351,381,388, 401,433,441, 455,465	6.1,14,22, 35,61.1,66B, 68.1,109,171, 175.1,184,205, 207,216,217, 219,225B,244.1, 249.1,263,270.1, 285,288,289, 300,305,322, 341,436,437, 452,454,470	13,16,79, 172,173.1,181, 190,210,212, 220.3,226,228, 234,241,247, 254,263.1,267, 272,274.1,275.1, 277.2,284,303.1, 314.1,319,324, 352,438,442, 460,469.1	9,28,34, 46,47,55, 68.2,175,186, 191,200,204, 208,215,220.1, 239,250,252, 265,266,280.1, 294,305.1,310, 338,356,368, 427.1,432
No., total(T)	7	31	34	33	32	29
QSOs(Q)	5	7	7	8	6	10
N.gals(N)	0	1	2	2	2	0
r.gals(R)	2	21	24	15	16	9
unident.(U)	0	2	1	8	8	10

α_{178}^{1400}, range	(-.15,-.48)	(-.50,-.73)	(-.74,-.82)	(-.83,-.88)	(-.89,-.99)	(-.99,-1.31)
α_{178}^{1400}, mean	-0.33±0.05	-0.65±0.01	-0.78±0.01	-0.86±0.01	-0.94±0.01	-1.08±0.02
$f(>S_o, m_v<17.6)$		15/31	17/34	9/33	3/32	5/29
$f(>S_o, z<0.2)$(T)		12/31	16/34	9/33	2/32	2/29
$f(>S_o, z<0.2)$(R+U)		11/23	15/25	9/23	1/24	2/19
$f(>S_o, z<1)$(Q)	4/5	7/7	3/7	4/8	2/8	3/10
$f(>S_o, P<10^{27\cdot2})$						
(T)		11/31	15/34	4/33	1/32	2/29
(R+U)		10/23	14/25	4/23	1/24	2/19
$f(>S_o, P<10^{28\cdot7})$ (Q)	3/5	4/7	2/7	4/8	1/6	2/10
$f(>S_o, \theta>35'')$		16/31	16/34	14/33	15/32	12/29
$z_{20\%}$ (R+U)		0.03	0.05	0.08	0.29	0.38
$z_{30\%}$ (R+U)		0.06	0.08	0.17	0.45	0.60
z,mean (Q)	0.82±0.07	0.71±0.09	0.84±0.18	1.05±0.19	0.98±0.15	1.23±0.19
z, median (Q)	0.86	0.69	1.03	0.96	1.04	1.11

178 MHz flux densities greater than S_0 with angular sizes larger than θ_0.

After discussing our source samples in Sect. 2 we shall examine the observed behaviour of the above fractions in Sect. 3. In Sect. 4 the fractions are evaluated theoretically for an expanding Friedman universe, and in Sect. 5 these theoretical results are compared with the empirical behaviour found in Sect. 3. Although the detailed results are sensitive to the input assumptions and are intended to be illustrative only, the comparison provides useful information regarding the spectral dependence of the evolution and luminosity of radio sources. Our principal conclusions are summarized in Sect. 6.

2. The Source Samples

a) The 3C *Sample*

We have taken sources with $S_{178} > 10$ Jy, $\delta \geqq 10°$ and $|b| \geqq 10°$. This comprises a total of 166 sources all of which have been mapped by the Cambridge 5 km telescope (Jenkins et al., 1977). The spectral indices were calculated from flux densities in Kellermann et al. (1969) corrected to the flux scale of Véron et al. (1974). The identification apparent magnitude and redshift data were taken from Smith et al. (1976) with a few additions communicated by Spinrad (1978). Of the 166 sources, 7 have $\alpha_{178}^{1400} > -0.5$. We have divided the remaining sources into 5 roughly equal groups in descending order of α_{178}^{1400}. The sources are listed in Table 1 together with some relevant properties of the sample.

b) The 4C *Sample*

We consider a total of 107 representative steep spectrum 4C sources, all of which have been observed with the Westerbork Synthesis Radio Telescope (WSRT). They have $S_{178} > 2$ Jy, $\delta \geqq 20°$, and $|b| \geqq 15°$, with values of α_{178}^{1415} ranging from -0.7 to -1.3. There are two subsamples. The first, observed by Conway et al. (1977) (CBV), had "normally" steep spectra ($-0.71 > \alpha_{178}^{1415} > -1.05$), and the second, from TMW, had

Table 2. The 4C sample according to α_{178}^{1415}

	CBV		TMV	
α_{178}^{1415}, range	(-0.71, -0.89)	(-0.90, -1.05)	(-0.95, -1.10)	(-1.11, -1.35)
Sources, 4C	38.03, 25.03, 25.07, 29.05, 34.06, 27.07, 29.08, 26.12, 29.25, 29.31, 34.30, 25.29, 39.29, 25.33, 34.33, 35.24, 25.36, 29.46, 37.34, 27.26, 28.35, 37.44, 34.42, 30.29, 34.43, 26.49, 29.50, 27.40, 37.52, 35.53, 36.47, 39.73, 37.69, 27.54	26.08, 35.05, 28.06, 29.08, 35.06, 34.13, 35.15, 37.18, 35.18, 29.32, 39.26, 26.29, 26.31, 33.38, 26.32, 38.31, 25.37, 37.33, 26.37, 38.33, 37.35, 38.34, 38.35, 38.36, 33.36, 25.48, 30.30, 37.49, 38.43, 24.53, 33.57, 37.67, 29.69	50.18, 57.14, 54.14, 45.16, 61.19, 42.27, 60.14, 50.31, 26.38, 26.39, 61.28, 59.20, 48.38, 23.38, 42.39, 46.32, 55.35, 26.62	46.01, 46.12, 41.17, 47.25, 53.19, 40.29, 24.28, 24.33, 59.22, 53.38, 56.25, 42.44, 48.45, 40.36, 25.36, 40.46, 28.58
No., total	34	33	18	17
$f(>S_o, m_v<19.4)^+$	0.380	0.200	0.180	0.035
$f(>S_o, \theta>20'')$	19/34	18/33	7/18	4/15

+Allowing for the effect of chance coincidences as described by TMW.

very steep spectra ($-0.95 > \alpha_{178}^{1415} > -1.28$). Both of these subsamples were observed in the same observing period and the calibration and reduction were performed in identical manners. Flux densities and spectral indices are placed on the scale of Véron et al. (1974). For the purposes of our investigation we divided each of the two subsamples into two roughly equal groups in descending order of spectral index. Details of the sample are given in Table 2.

For the 4C sources flux densities have been measured at only three frequencies, 178, 1415, and 4995 MHz. Since the 1415 MHz flux densities are in general much better determined, we shall use α_{178}^{1415} in our study. However, most of the effects we shall discuss are present to the same extent if one examines α_{178}^{4995}.

3. The Fractions – Observations

a) Apparent Magnitude

For each of the spectral groups (five for the 3C sample and four for the 4C sample) we calculated $f(>S_0, <m_0)$. This is merely the number of sources whose optical apparent magnitude is brighter than m_0 divided by the total number of sources in the group. (S_0 is the limiting flux density, i.e. 10 Jy for the 3C sources and 2 Jy for the 4C sources).

For the 4C sources the limiting magnitude $m_0 = 19.4$ correponds to the cut-off of the Palomar Sky Survey. For comparison purposes we chose a limiting magnitude of $m_0 = 17.6$ for the 3C sources, where the difference of 1.8 mag merely corresponds to the ratio between the mean 3C and 4C flux densities.

Figure 1 shows $f(>S_0, <m_0)$, plotted against the spectral index, α_{178}^{1415}. Note the striking agreement between the behaviour of the 3C and 4C sources. This suggests that there is a strong correlation between apparent magnitude and spectral index. This correlation persists if instead of α_{178}^{1415} one uses the spectral index determined over any frequency range between 178 and 5000 MHz.

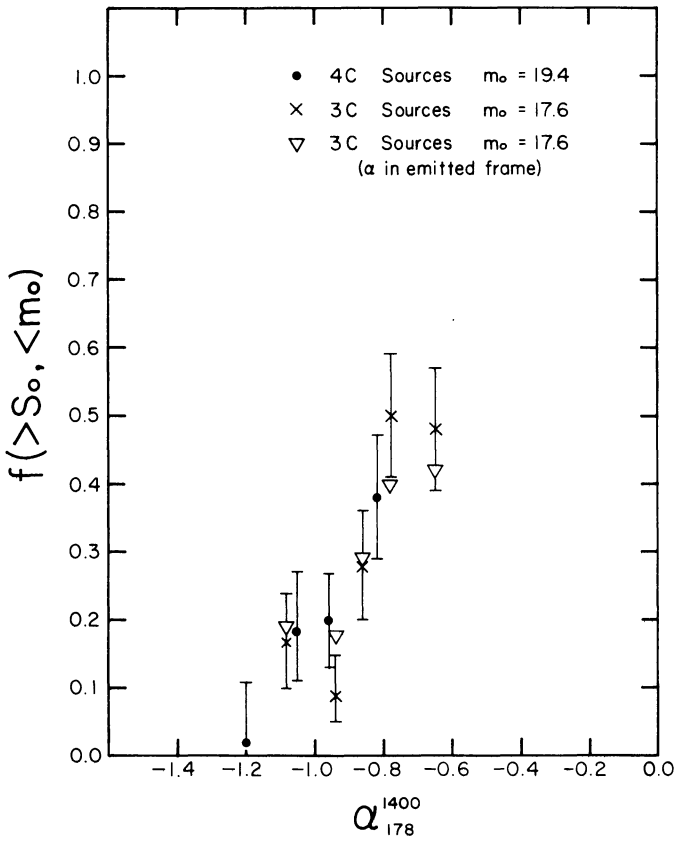

Fig. 1. Fraction of sources with optical counterparts brighter than m_0 plotted against the observed meter wave spectral index (α_{178}^{1400} for the 3C sources and α_{178}^{1415} for the 4C sources). Also shown are the fractions corresponding to the case where the spectral index is evaluated in the emitted frame (see text)

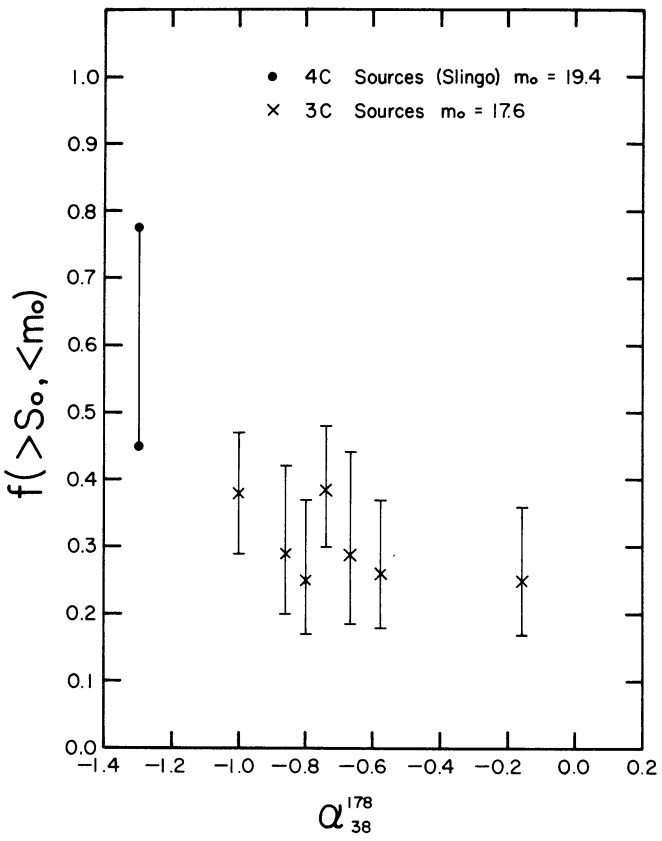

Fig. 2. Fraction of sources with optical counterpart brighter than m_0 plotted against the decameter-wave spectral index α_{38}^{178}. The identified fraction of Slingo's 4C sample is discussed by TMW and lies between the limits shown here

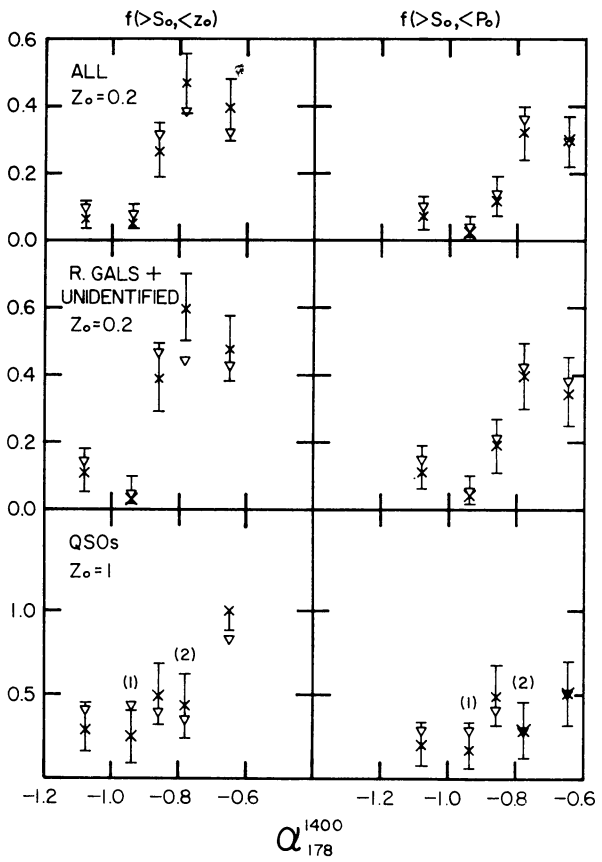

Fig. 3. Fraction of sources with (a) redshifts smaller than z_0 and (b) monochromatic 178 MHz luminosities smaller than P_0 plotted against the observed meter wave spectral index. P_0 is given by Eq. (7) with S_v = 10 Jy, the limiting 3C flux density. The figures in parentheses for QSOs represent the number of unknown redshifts for the group. The open triangles indicate the fractions obtained when the spectral index is evaluated in the emitted frame (see text)

However, a marked difference is found if a spectral index below 178 MHz is used. From Fig. 2, which shows $f(>S_0, <m_0)$ plotted against α_{38}^{178}, it is apparent that the correlation of Fig. 1 is washed out for decameter wave spectra. Thus the difference pointed out by TMW between steep spectrum 4C sources, selected above and below 178 MHz, is also present in the 3C source sample.

These differences are probably due to a combination of two effects. First, a large number of the more distant and luminous steep spectrum sources must have spectra which become optically thick at frequencies close to 100 MHz. Secondly, there is a population of less luminous relatively nearby sources (some identified with rich clusters) which have very steep spectrum components that dominate below 178 MHz.

b) Redshift and 178 MHz *Luminosity*

Since for steep spectrum sources, radio galaxies are the dominant population, Fig. 1 argues for a relation between the meter-wave spectral index and the redshift of radio galaxies. For the 3C sample, redshifts are available for the majority of sources, so we can examine the redshifts and monochromatic luminosities as functions of the spectral index.

In Fig. 3 $f(>S_0, <z_0)$ and $f(>S_0, <P_0)$ are plotted against α_{178}^{1415} for (i) the whole 3C sample, (ii) the radio galaxies and unidentified sources together, and (iii) the quasars. Since it is likely that all sources with $z < 0.2$ have been identified, we take $z_0 = 0.2$ as the limiting redshift. In the case of the quasars, only 3 of the 43 have unknown redshifts so we have taken $z_0 = 1$ to improve the statistics. We have assumed that the three unknown quasar redshifts, none of which occur in extreme spectral index groups, are all greater than 1. With a Hubble Constant of 55 km s^{-1} Mpc^{-1} and $q_0 = 0.5$, at our flux limit of 10 Jy, $z_0 = 0.2$ and 1.0 would correspond to $P_0 \sim 10^{27.2}$ and $10^{28.7}$ W Hz^{-1} respectively. Hence our limiting luminosities.

There are seven N-galaxies in our 3C sample. These have several of their properties intermediate between quasars and typical radio galaxies, so it is not clear whether they should be included in category (ii) or category (iii). We have therefore omitted them entirely from both categories and from the comparison of the quasar with the radio galaxies that follows.

From Fig. 3 it follows that sources with steeper spectra tend to have larger redshifts and 178 MHz monochromatic luminosities. The effect is present in the same sense for both radio galaxies and quasars.

The redshift relation is shown in a different form in Fig. 4 which is a plot of redshift against spectral index for (i) the

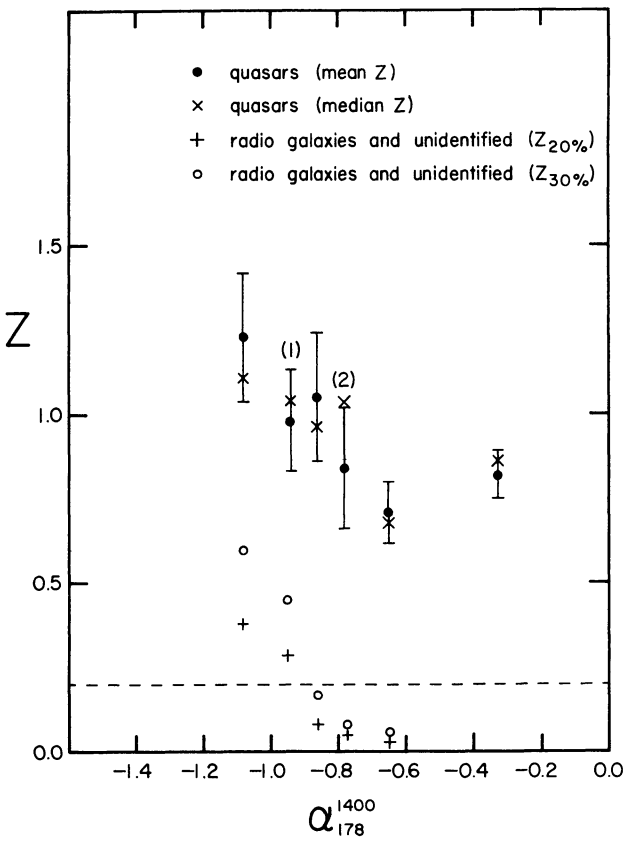

Fig. 4. Redshift plotted against the meter wave spectral index. For QSOs the number of unknown redshifts in a group is shown in parentheses

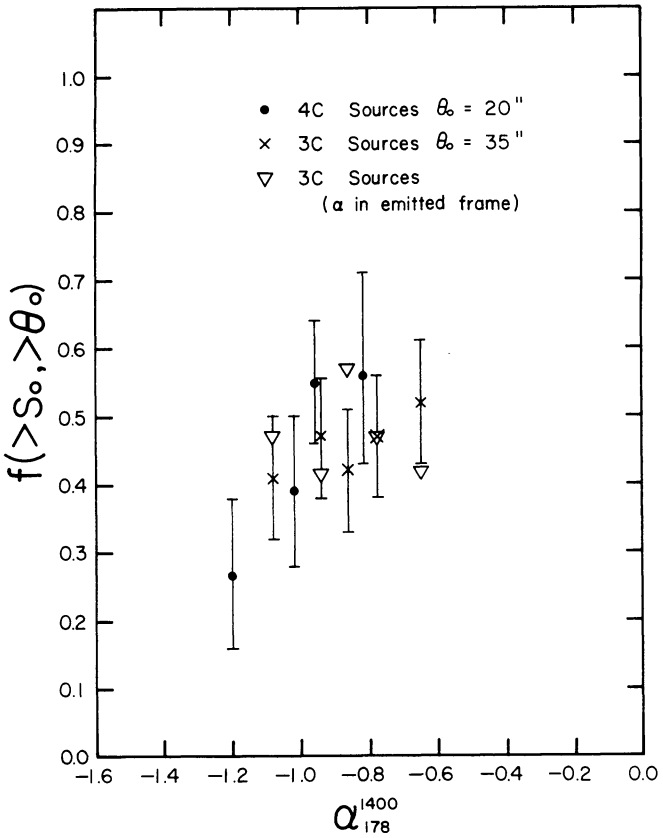

Fig. 5. Fraction of sources with angular size greater than θ_0 plotted against the meter-wave spectral index

quasars and (ii) the radio galaxies and unidentified sources. For the quasars (only 3 missing redshifts) we show the mean and median redshifts whereas for the radio galaxies and unidentified sources we use the 20th and 30th percentiles of redshift, again assuming the missing redshifts to be in excess of 0.2. Note that both for the radio galaxies and unidentified sources and for the quasars, steeper meter wave spectra are associated with larger redshifts. Since there are several reasons for assuming that almost all the unidentified sources are radio galaxies, we conclude that the spectral index–redshift correlation is present both in radio galaxies and quasars separately.

c) Angular Sizes

In Fig. 5 we show $f(>S_0, >\theta_0)$, the fraction of sources having angular sizes larger than a limiting value, plotted against the spectral index, α_{178}^{1415}. For the 4C sources our limiting angular size $\theta_0 = 20''$ corresponds to the limiting resolution of the WSRT at 1415 MHz. In order to compare the two samples we chose a limiting angular size of $\theta_0 = 35''$ for the 3C sources. The ratio 35/20 corresponds to the square root of the ratio of the median 3C and 4C flux densities and assumes Euclidean behaviour of the angular size–flux density relation.

Note that for the 4C sources there is a tendency for the steeper spectra to correspond to smaller angular sizes. Such an effect is consistent with the steeper spectrum sources being on average further away as indicated by Figs. 1, 3, and 4.

d) Spectral Indices in the Emitted Frame

The fractions in Figs. 1–5 are plotted as functions of the *observed* spectral index

$$\alpha_{178}^{1400} = \log\{S(1400)/S(178)\}/\log(1400/178).$$

It is more relevant to consider them as a function of spectral index measured over a constant *emitted* frequency range but this is impossible since a large number of the sources have unknown redshifts. To estimate what effect the use of the emitted spectral indices would have, we recalculated the fractions for the 3C sources as a function of

$$\alpha_{178}^{1400}\ (\text{emitted}) = \log\{S(1400/(1+z))/S(178/(1+z))\}/\log(1400/178),$$

assuming the unknown redshifts to be 2. The spectra were interpolated to the emitted frame using flux densities from Kellermann et al. (1969).

The results are also shown in Figs. 1, 3, and 5. Note that since many of the unknown redshifts (optically faint and unidentified sources) might be considerably smaller than 2, the plotted point corresponding to the emitted case is probably an extreme value. In practice the actual fractions should lie between the "observed" and "emitted" values.

The only fraction to be significantly altered is $f(>S_0, >\theta_0)$ involving the angular size. For the 3C sources the weak trend as a

function of observed spectral index is no longer present. However, taking into account the 4C data, we believe that there is still strong evidence that the steeper spectra sources are smaller on average.

e) Selection Effects

The first question that naturally arises is whether Figs. 1, 3, 4, and 5 could be produced by selection effects? This does not seem likely since most selection effects are independent of spectral index. There are, however, two effects that are worthy of consideration.

If source structures become more nonuniform with steeper spectra (e.g. the flux ratios of double sources become more unequal) one might (i) miss identifications for steeper spectrum sources and (ii) measure smaller angular sizes for these sources. However, an examination of the 3C sample for which excellent structural information is available does not reveal any such effect.

Another source of influence, particularly in Fig. 5, might be the inherent uncertainty in the integrated spectral indices for some of the very large sources. There are only 4 sources in the 3C sample with angular sizes in excess of $\sim 10'$. Some of these may have been inadvertently placed in the wrong spectral index group, but they are unlikely to have been misplaced by more than one group. The total influence of this effect on the general behaviour shown in Figs. 1–5 would be negligible.

The structure and spectra of sources in the 3C and 4C samples have been determined with different instruments and the optical identifications have been carried out independently by different workers. We therefore believe that the good agreement between the behaviour of the two samples shown in Figs. 1 and 2 is strong evidence for the reality of the correlations.

4. Calculation of the Fractions

In order to interpret the variations of such fractions as $f(<S_0, <z_0)$ and $f(>S_0, <P_0)$ with spectral index α, we must first make several assumptions about the global distribution of radio sources. This permits us to relate the α dependence of the observed fractions to the spectral index dependence of the luminosity function and evolution of the radio sources. In particular, we assume that the proper density of sources at redshift z with emitted spectral power (at emitted frequency ν) lying between P_ν and $P_\nu + dP_\nu$ and with projected linear size lying between L and $L + dL$ is

$$\rho(P_\nu, z, L)dP_\nu dL = \rho_0(1+z)^3 F(z)\phi(P_\nu)\psi(L)dP_\nu dL, \quad (1)$$

where ρ_0 represents the present density of sources. Inherent in Eq. (1) is the assumption that z, P_ν and L are all uncorrelated. However, in interpreting Fig. 3, we shall essentially integrate over L and remove any assumptions about its correlation.

For the density evolution, we assume $F(z)$ to be of the form

$$F(z) = (1+z)^n \theta(z_u - z) \quad (2)$$

(Longair, 1966) where z_u is the cutoff redshift and $\theta(x)$ is the Heaviside function, which has value unity when $x > 0$ and is zero otherwise. We assume the radio spectral luminosity function $\phi(P_\nu)$ to be a power law as well:

$$\phi(P_\nu) = kP_\nu^{-\gamma}\theta(P_\nu - P_L)\theta(P_u - P_\nu). \quad (3)$$

Finally, following Kapahi (1975) we may use

$$\psi(L) = (2/L_u)\{\arccos(L/L_u) - (L/L_u)\ln[1 + (L_u^2/L^2 - 1)^{1/2}]\}. \quad (4)$$

This corresponds to a linear distribution of actual physical (non-projected) sizes, all randomly oriented, which has an upper cut-off at L_u and decreases linearly with physical size. Since the mean linear size of radio sources is observed to decrease with redshift (Wardle and Miley, 1972; Kapahi, 1975) we should allow for this by taking

$$L_u = \tilde{L}_u(1+z)^{-\xi} \quad (5)$$

in which case $\psi(L)$ becomes a function of z as well.

In general, the parameters n, z_u, k, γ, P_L, P_u, $\tilde{L}_u$, and ξ can all be functions of spectral index α. In practice, at least for the data here, the statistics are not good enough to fit more than a few parameters.

For a luminosity distance defined by (Mattig, 1958)

$$D = (c/H_0 q_0^2)\{q_0 z + (q_0 - 1)[(1 + 2q_0 z)^{1/2} - 1]\} \quad (6)$$

and the K correction determined by the spectral index α, the radiated spectral power is related to the observed flux density S_ν at the same frequency by

$$P_\nu = 4\pi S_\nu D^2/(1+z)^{1+\alpha}, \quad (7)$$

The projected linear size L is then also related to the angular size and luminosity distance:

$$L = \theta D(1+z)^{-2}. \quad (8)$$

One should note that the weakest sources, those with emitted power P_L, appear within a survey down to flux density S_0 only if they have redshift less than

$$z_c \cong (H_0/c)(P_L/4\pi S_0)^{1/2}. \quad (9)$$

The fractions $f(>S_0, <z_0)$ and $f(>S_0, <P_0)$, are both related to the same source parameters n, γ, z_u, P_u, and P_L. We shall therefore attempt to fit both these fractions simultaneously.

Using the Robertson-Walker metric and the Friedman universe, it follows from Eq. (1) that the number of sources between z and $z + dz$, with emitted power between P_ν and $P_\nu + dP_\nu$, is

$$dN = 4\pi\rho_0 c H_0^{-1} D^2 (1+z)^{-3}(1+2q_0 z)^{-1/2} F(z)\phi(P_\nu)dz dP_\nu, \quad (10)$$

where q_0 is the deceleration parameter.

Hence,

$$N(>S_0, <z) = \int_0^z \int_{P^*}^{P_u} dN \quad (11)$$

and

$$N(>S_0, <P_0) = \int_0^{z_0} \int_{P^*}^{P_0} dN \quad (12)$$

where

$$P^* = \max\{P_L, 4\pi S_0 D^2/(1+z)^{1+\alpha}\}. \quad (13)$$

z_0 is the solution of Eq. (7) with $S_\nu = S_0$ and $P_\nu = P_0$. z_0 corresponds to the redshift at which a source with luminosity P_0 just appears in the survey.

In Eq. (11) it is assumed that sources with emitted power P_u can be observed at least out of the cutoff redshift z_u. The fractions then become

$$f(>S_0, <z) = \frac{J_2(z_c, P_L) + J_1(z) - J_2(z, P_u)}{J_2(z_c, P_L) + J_1(z_u) - J_2(z_u, P_u)} \quad (14)$$

and

$$f(>S_0, <P_0) = \frac{J_1(z_0) + J_2(z_c, P_L) - J_2(z_0, P_0)}{J_1(z_u) + J_2(z_c, P_L) - J_2(z_u, P_u)}, \quad (15)$$

where

$$J_1(z) = \int_{z_c}^{z} dz \left(\frac{H_0 D}{c}\right)^2 \frac{(1+z)^{n-3}}{(1+2q_0 z)^{1/2}} \left[\left(\frac{H_0 D}{c}\right)^2 (1+z)^{-(1+\alpha)}\right]^{1-\gamma} \quad (16)$$

while

$$J_2(z, P) = \left(\frac{P H_0^2}{4\pi S_0 c^2}\right)^{1-\gamma} \int_0^z dz \left(\frac{H_0 D}{c}\right)^2 \frac{(1+z)^{n-3}}{(1+2q_0 z)^{1/2}}. \quad (17)$$

For $q_0 = 0$ or $\frac{1}{2}$ it is easy to integrate $J_2(z, P)$ in closed form. For noninteger γ, $J_1(z)$ is most easily evaluated numerically.

Note that since $D \cong cz/H_0$ for small z, the integrand of Eq. (16) goes roughly as $z^{2(2-\gamma)}$ for small z, which leads to a diverging integral when $\gamma \geqq 2.5$. This corresponds to the well-known critical luminosity function encountered in studies of the radio source counts (von Hoerner, 1973). It is also noteworthy that when $z_0 = z$, then necessarily $f(>S_0, <z) > f(>S_0, <P_0)$.

In order to interpret the data, the ideal approach would be to integrate Eq. (10) once, and for each spectral index fit the observed differential number counts dN/dz and dN/dP_ν as functions of z and P_ν respectively, but this is impractical. First, at this time there are not enough sources to bin in both spectral index and one other variable. Secondly, for a large number of the sources only limits are available for the observed parameters of interest. Therefore, the integrated fractions which are independent of k and ρ_0, are most useful. For each spectral index α, the two fractions $f(>S_0, <z)$ and $f(>S_0, <P_0)$ can serve to determine only two parameters, although n, γ, z_u, P_L, and P_u are all unknown. We shall therefore choose z_u, P_L, and P_u to be independent of α and determine the spectral index dependence of the parameters n and γ which characterize the source evolution and luminosity functions.

Following Kapahi (1975), we shall assume $z_u = 3$ and $P_L = 10^{24}$ W Hz^{-1}. A spectral dependence of z_u will then induce an α-dependent error in our determination of n, the source evolution. Equivalently, an error in our estimate of P_L will result in a change in γ, the luminosity function index. Finally, since $\gamma \gtrsim 2$, there are very few high luminosity sources, the fractions depend only weakly on P_u, and we therefore take $P_u = \infty$.

5. Discussion

The striking variation of the apparent magnitude fractions shown in Fig. 1 shows that some property of steep spectrum radio sources changes strongly as a function of the spectral index measured above 178 MHz. Although in principle a dependence of optical luminosity on the radio spectral index could explain the effect, the most straightforward explanation is that the sources with the steepest spectra are on average more luminous radio emitters and located further away. This hypothesis is supported by the data on redshift and luminosity distributions plotted in Fig. 3. Previous authors (e.g. Heeschen, 1960; Véron et al., 1972; Macleod and Doherty, 1972; Bridle et al., 1972) have drawn attention to a possible increase in radio luminosity with steepening spectra, but we believe that the diagram in Fig. 1 is the most convincing demonstration of this correlation to date.

In order to investigate the cause in more detail, we have applied the analysis outlined in Sect. 4 to the data on 3C sources shown in Fig. 3. To reduce the statistical uncertainties, it would have been preferable to have treated both the 3C and 4C samples, but since redshifts are unavailable for most of the 4C sources, this was not possible.

The fractions $f(>S_0, <z_0)$ and $f(>S_0, <P_0)$ given by Eqs. (14) and (15) were fitted to the five pairs of points corresponding to the different spectral indices shown in Fig. 3. For each pair we plotted the range of the evolution and luminosity function exponent n and γ which are allowed by the uncertainties in the observed fractions. The analysis was carried out with $z_0 = 0.2$, $P_0 = 10^{27.2}$ W Hz^{-1} for all sources and for $z_0 = 1.0$, $P_0 = 10^{28.7}$ W Hz^{-1} for quasars alone. In each case, this resulted in two narrow strips of roughly equal slope in the (n, γ) plane, an example of which is shown in Fig. 6. The two fractions thus measure a linear combination of n and γ much more accurately than either n or γ. Because of this asymmetry in the error contours, it is useful to consider the lines in the (n, γ) plane roughly defined by the error strips. Writing this as

$$A = n - B\gamma \quad (18)$$

we find that for both $z_0 = 0.2$ ($B = 9.5 \pm 0.5$) and for $z_0 = 1.0$ ($B = 6.7 \pm 0.2$) there is only slight variation in the slope B

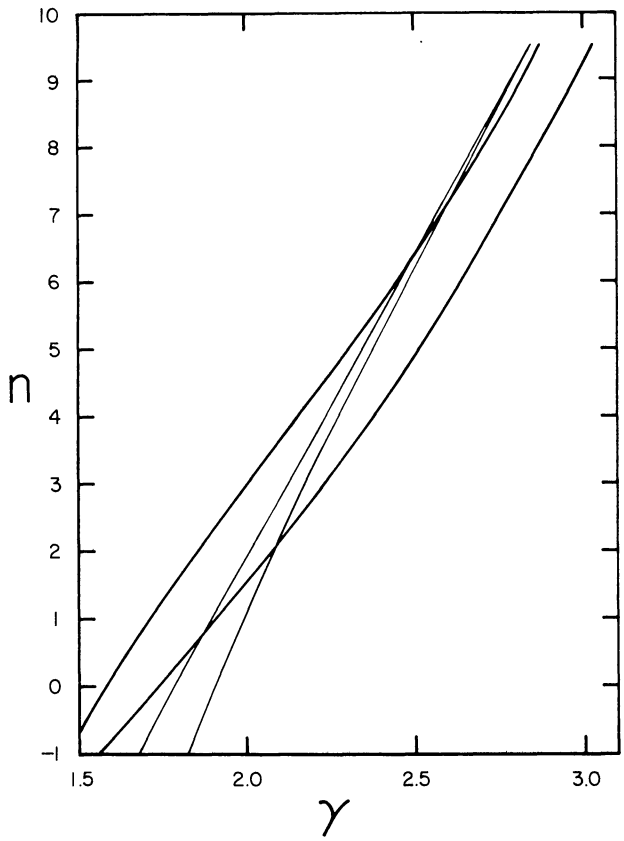

Fig. 6. Error strips in the evolution (n) – luminosity function (γ) plane for $\alpha_{178}^{1400} = -0.86$. The thick lines refer to QSOs ($z_0 = 1$) and the thin lines refer to all sources ($z_0 = 0.2$)

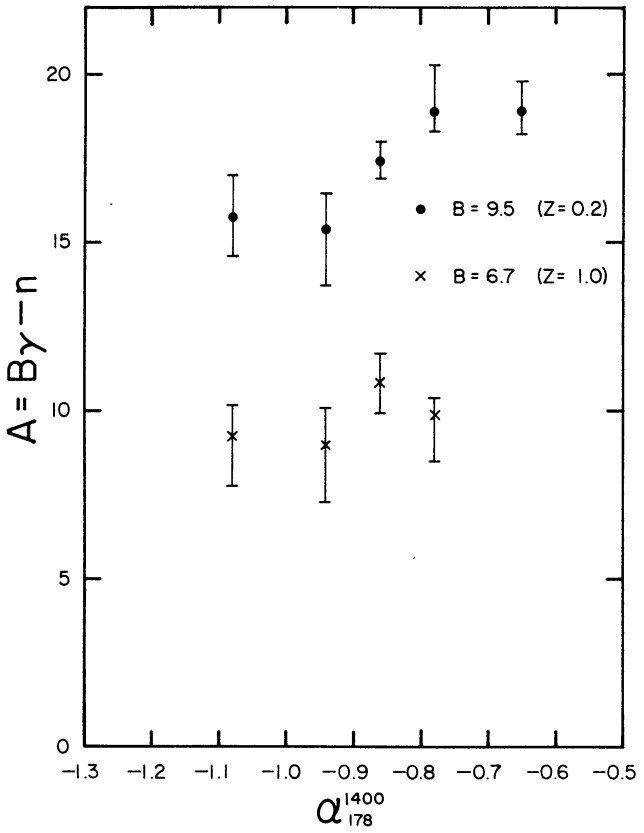

Fig. 7. Deduced values of $B\gamma - n$ (see Eq. 18) plotted against the meter-wave spectral index

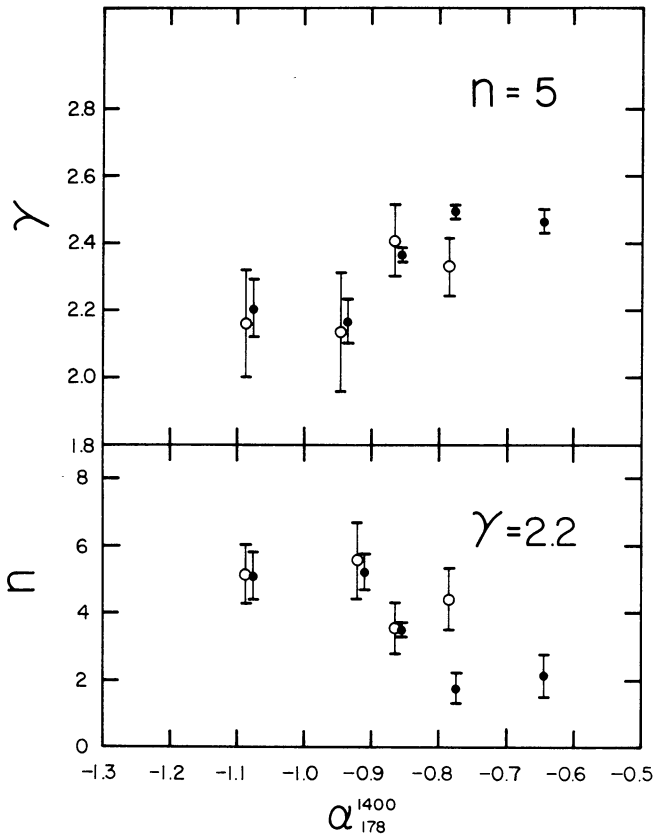

Fig. 8. Deduced values of γ (above) and n (below) plotted against the meter-wave spectral index assuming that n (above) or γ (below) are independent of spectral index. The filled circles correspond to $z_0 = 0.2$ and the open circles to $z_0 = 1.0$ (see text)

among the 5 spectral points. Figure 7 shows the result of taking B to be different constants for the two values of z_0 and plotting the intercept A as a function of spectral index. Note the definite change in A with spectral index for $z_0 = 0.2$. The statistical uncertainties are of course larger for $z_0 = 1$ and in this case the flattest spectral index pair was impossible to fit consistently. This extreme group might well include some flat spectrum compact sources which contaminate our sample of steep spectrum extended sources.

The above analysis was carried out for a deceleration parameter of $q_0 = \frac{1}{2}$. Taking $q_0 = 0$ raises the absolute values of A and B somewhat but does not affect the trend shown in Fig. 7 significantly.

From this analysis therefore, it is not possible to answer whether a dependency on spectral index of either the luminosity function or evolution function alone can explain our results. It is, however, interesting to consider the range of variation of γ and n with spectral index which is required if each of these parameters is successively held constant. The results shown in Fig. 8 show that a relatively modest flattening of the luminosity function for steeper spectrum sources is needed while a large change in density evolution would be required to fit the data.

The actual values are intended to be illustrative only and the reader should bear in mind the large number of simplifying assumptions that were made in Sect. 4 and that usually go into this type of analysis. For example, variations in the luminosity function would probably manifest themselves as changes in the shape and cut-off as well as in the slope γ. Also the $(1 + z)^n$ evolution function is almost certainly a gross oversimplification of reality.

We have not applied the method outlined in Sect. 4 to our angular size data in Fig. 5. As we have seen in Sect. 3, the statistics are poorer. Also, Kapahi (1975) has shown that both linear size and density evolution are required to account for the behaviour of the overall $N(\theta)$ relation. We felt that the resultant extra parameters involved, and their possible interrelationships. would make it impossible to derive any useful quantitative results from Fig. 5. The trend for steep spectrum sources to be smaller is however consistent with our suggestion that either the luminosity function is flatter and/or the evolution is strongest for the steepest spectrum sources.

The results shown in Fig. 8 show that our correlations are more sensitive to a small change in γ than in n. Further evidence that the luminosity function rather than source evolution is the culprit is provided by the fact that several authors (e.g. Schmidt, 1977) have found similar behaviour in evolution ($n \sim 5$) for both the radio quiet QSOs and the steep spectrum quasars. This would be rather coincidental if the evolution function varied greatly within the steep spectrum quasar sample. The dependence of either the luminosity function or the evolution function on spectral index has important consequences for models of radio sources. In recent years there

has been mounting evidence that acceleration of the radiating relativistic electrons takes place in the radio lobes, possibly at the boundary of the source with the ambient medium. Since the intergalactic medium will most likely change systematically with redshift, the present work favours acceleration mechanisms in which the resultant radio luminosity and spectral index depend strongly on the properties of this medium.

6. Conclusions

1. For steep spectrum radio sources there is a strong relationship between the apparent magnitude and the spectral index measured above 178 MHz (Fig. 1).

2. In addition, the radio spectrum correlates with the redshift (Figs. 3 and 4), the radio luminosity (Fig. 3), and the angular size (Fig. 5).

3. Similar behaviour is observed for both radio galaxies and quasars (Figs. 3 and 4), furnishing another argument that their redshifts have the same origin.

4. The correlations are most likely due to variations of the radio luminosity and/or density evolution functions with spectral index.

5. The method for analysing the observed fractions outlined here is a useful tool for investigating such effects but does not yet allow us to establish whether they are due to variation in luminosity or evolution.

6. The similar evolutionary behaviour of radio quiet and steep spectrum radio loud QSOs is slight evidence that evolution is constant and therefore, changes in the radio luminosity function are responsible for the observed effects.

7. The apparent magnitude spectral index correlation does not hold for spectral indices measured below 178 MHz (Fig. 2). This suggests that there are two separate populations of steep spectrum radio sources – the low frequency ultra steep spectrum sources which are often identified with nearby clusters, and the high luminosity steep spectrum sources predominantly associated with distant radio galaxies.

8. Selecting subsamples according to spectral index should narrow the dispersion in those statistical analyses of steep spectrum radio sources which involve luminosity (e.g. source counts).

Acknowledgements. We thank Hy Spinrad for access to his data prior to its publication and Harry van der Laan for useful suggestions. Gordon Robertson, Malcolm Longair, and Sebastian von Hoerner made helpful comments on the manuscript. GKM acknowledges a travel grant from the Netherlands Organization for the Advancement of Pure Research (Z.W.O.) and support from the Martin Kellogg Fund. GRB was supported in part by NSF grant AST 74-193787-A02.

Note added in proof. Dr. I. Browne has pointed out that the identification of 4C 61.19 was missed by Tielens et al. (1979). This was due to an error in the overlay used for this source. 4C 61.19 is an 18 m QSO with a redshift of 0.862 (Wills, D., Wills, B. J.: 1976, Astrophys. J. Suppl. **31**, 143). The addition of this extra identification ($\alpha_{178}^{1415} = -1.03$) to the TMW sample has no significant effect on the results presented here.

References

Bridle, A.H., Kesteven, M.J.L., Guindon, B.: 1972, *Astrophys. Letters* **11**, 27

Conway, R.G., Burn, B.J., Vallee, J.P.: 1977, *Astron. Astrophys. Suppl.* **27**, 155

Heeschen, D.: 1960, *Publ. Astron. Soc. Pacific* **72**, 368

Hoerner, S. von: 1973, *Astrophys. J.* **186**, 741

Jenkins, C.J., Pooley, G.G., Riley, J.M.: 1977, *Monthly Notices Roy. Astron. Soc.* **84**, 61

Kapahi, V.K.: 1975, *Monthly Notices Roy. Astron. Soc.* **172**, 513

Kellermann, K.I., Pauliny-Toth, I.I.K., Williams, P.J.S.: 1969, *Astrophys. J.* **157**, 1

Longair, M.S.: 1966, *Monthly Notices Roy. Astron. Soc.* **133**, 421

Macleod, J.M., Doherty, L.H.: 1972, *Nature* **238**, 88

Mattig, W.: 1958, *Astron. Nachr.* **284**, 109

Schmidt, M.: 1977, *Proc.* IAU *Symposium* No. 74, 259, Radio Astronomy and Cosmology, D. L. Jauncey, Ed.

Slingo, A.: 1974, *Monthly Notices Roy. Astron. Soc.* **168**, 307

Smith, H.E., Spinrad, H., Smith, E.O.: 1976, *Publ. Astron. Soc. Pacific* **88**, 621

Spinrad, H.E.: 1978, private communication

Tielens, A.G.G.M., Miley, G.K., Willis, A.G.: 1978, *Astron. Astrophys. Suppl.* (in press)

Véron, M.P., Véron, P., Witzel, A.: 1972, *Astron. Astrophys.* **18**, 82

Véron, M.P., Véron, P., Witzel, A.: 1974, *Astron. Astrophys. Suppl.* **13**, 1